



UNIVERSITY OF LEEDS

This is a repository copy of *Elemental distribution within the long-period stacking ordered structure in a Mg-Gd-Zn-Mn alloy*.

White Rose Research Online URL for this paper:
<http://eprints.whiterose.ac.uk/131220/>

Version: Accepted Version

Article:

Li, J, Hage, FS, Zhong, X et al. (5 more authors) (2017) Elemental distribution within the long-period stacking ordered structure in a Mg-Gd-Zn-Mn alloy. *Materials Characterization*, 129. pp. 247-251. ISSN 1044-5803

<https://doi.org/10.1016/j.matchar.2017.05.008>

(c) 2017, Elsevier Inc. This manuscript version is made available under the CC BY-NC-ND 4.0 license <https://creativecommons.org/licenses/by-nc-nd/4.0/>

Reuse

This article is distributed under the terms of the Creative Commons Attribution-NonCommercial-NoDerivs (CC BY-NC-ND) licence. This licence only allows you to download this work and share it with others as long as you credit the authors, but you can't change the article in any way or use it commercially. More information and the full terms of the licence here: <https://creativecommons.org/licenses/>

Takedown

If you consider content in White Rose Research Online to be in breach of UK law, please notify us by emailing eprints@whiterose.ac.uk including the URL of the record and the reason for the withdrawal request.

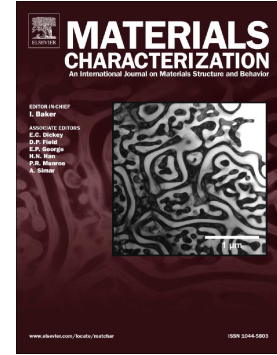


eprints@whiterose.ac.uk
<https://eprints.whiterose.ac.uk/>

Accepted Manuscript

Elemental distribution within the long-period stacking ordered structure in a Mg-Gd-Zn-Mn alloy

Jiehua Li, Fredrik S. Hage, Xiangli Zhong, Yujuan Wu, Liming Peng, Sarah J. Haigh, Quentin M. Ramasse, Peter Schumacher



PII: S1044-5803(16)31402-4
DOI: doi: [10.1016/j.matchar.2017.05.008](https://doi.org/10.1016/j.matchar.2017.05.008)
Reference: MTL 8669
To appear in: *Materials Characterization*
Received date: 23 December 2016
Revised date: 7 May 2017
Accepted date: 9 May 2017

Please cite this article as: Jiehua Li, Fredrik S. Hage, Xiangli Zhong, Yujuan Wu, Liming Peng, Sarah J. Haigh, Quentin M. Ramasse, Peter Schumacher , Elemental distribution within the long-period stacking ordered structure in a Mg-Gd-Zn-Mn alloy, *Materials Characterization* (2017), doi: [10.1016/j.matchar.2017.05.008](https://doi.org/10.1016/j.matchar.2017.05.008)

This is a PDF file of an unedited manuscript that has been accepted for publication. As a service to our customers we are providing this early version of the manuscript. The manuscript will undergo copyediting, typesetting, and review of the resulting proof before it is published in its final form. Please note that during the production process errors may be discovered which could affect the content, and all legal disclaimers that apply to the journal pertain.

**Elemental distribution within the long-period stacking ordered
structure in a Mg-Gd-Zn-Mn alloy**

Jiehua Li^{1,2*}, Fredrik S. Hage³, Xiangli Zhong⁴, Yujuan Wu², Liming Peng², Sarah J.
Haigh⁴, Quentin M. Ramasse³, Peter Schumacher^{1,5}

¹ Institute of Casting Research, Montanuniversität Leoben, A-8700, Leoben, Austria

² National Engineering Research Center of Light Alloy Net Forming and State Key
Laboratory of Metal Matrix Composites, Shanghai Jiaotong University, 200240, Shanghai,
PR China

³ SuperSTEM Laboratory, SciTech Daresbury Campus, Keckwick Lane, Daresbury, WA4
4AD, UK.

⁴ School of Materials, The University of Manchester, Manchester M13 9PL, England, UK

⁵ Austrian Foundry Research Institute, Leoben, Austria

*Corresponding Author:

Post address: Institute of Casting Research, Montanuniversität Leoben, A-8700, Leoben,
Austria.

Tel.: +43-3842-402-3304; Fax: +43-3842-402-3302.

Email address: jie-hua.li@hotmail.com (Jiehua Li)

Abstract

High angle annular dark field scanning transmission electron microscope imaging and electron energy loss spectroscopy was used to elucidate the elemental distribution (Gd, Zn, Mn) within the long-period stacking ordered (LPSO) structure in a Mg-15Gd-0.8Zn-0.8Mn (wt %) alloy. While Gd and Zn enrichment was observed within the LPSO structure, no significant enrichment in Mn was observed. After averaging over a large region, a very weak Mn signal was resolved but no significant variations in Mn signal were observed over this region, suggesting that Mn is indeed present. These results provide useful information to support the future development of high performance Mg alloys.

Keywords: Magnesium alloys; Segregation; Long-period stacking ordered structure; High angle annular dark field (HAADF); Electron energy loss spectroscopy (EELS)

1. Introduction

Magnesium alloys have a great potential and have been widely used as important structural parts for automotive and aerospace applications due to their high specific strength [1]. However, compared with high performance Al alloys, the effect of precipitation hardening of Mg alloys is comparatively low due to the lower number density and volume fraction observed in conventional Mg alloys (i.e. AZ91, AM60, ZK60) [2]. Furthermore, the thermal stability of these precipitates (i.e. $Mg_{17}Al_{12}$ in AZ91) formed in conventional Mg alloys is relatively lower when compared with that formed in high performance Al alloys. Therefore, the application of these conventional Mg alloys has been limited to specific components that operate at temperatures below 150 °C due to the rapid degradation of the mechanical properties at elevated temperatures, especially the creep resistance. To date, some novel high performance Mg alloys (MRI230D, AS31, AJ62, AE44, WE43 and Elektron21 et al) have been developed for possible applications at elevated temperatures. For example, AJ62 alloy has been used for transmission cases together with Al alloys in engine blocks. WE43 alloy has been used for engine blocks in Formula1 in temperature ranges up to 350 °C. Even pistons have been made from Mg alloys or even metal matrix composites based on Mg. These novel high performance Mg alloys are mainly strengthened by precipitation hardening. Apart from the well-accepted precipitation hardening, the formation of long-period stacking ordered structure (LPSO) structures in Mg alloys containing a small amount of transition metals (TM) and rare earths (RE) is also promising for the further Mg development due to their excellent mechanical properties [3].

Different LPSO structures (i.e. 18R, 14H, 10H, 24R) have been reported in Mg-TM-RE alloys (where TM refers to Zn etc and RE refers to Y, Gd etc) [4, 5]. The majority of previous research studies have mainly focused on Mg-Zn-Y alloys but Mg-Gd-Zn alloys may also offer the potential for improved performance because of the facts that small additions of Zn (about 1 wt %) stimulate an age hardening response in Mg-Gd alloys and thereby Gd contents can be decreased to a level (about 6 wt %) much lower than that (higher than 15wt %) ordinarily associated with a significant ageing response [6]. The precipitation of γ type precipitates on $(0001)_{\text{Mg}}$ planes has been observed in a Mg-Gd-Zn alloy with low Gd and Zn concentrations (i.e. Mg-6Gd-1Zn-0.6Zr (wt %)), which was aged at low temperatures (200 °C - 250 °C) [7]. More recently, the γ' and γ'' phases were also observed in a Mg-2.5Gd-1Zn (at %) alloy aged at 225 °C, where Zn atoms were found to occupy some atomic sites in the center layer of the γ'' phase [8]. Furthermore, in Mg-Gd-Zn alloys with high Gd and Zn concentrations (i.e. Mg-12Gd-2Zn-0.6Zr (wt %)), the formation of stacking faults and the 14H phase on $(0001)_{\text{Mg}}$ were observed at intermediate and high temperatures (300 °C - 500 °C) [9]. By contrast, the β' [10], β_1 [10] and β phases [9] were observed at low temperatures (200 °C) [9]. Clearly, alloy composition (i.e. Gd and Zn concentrations as well as the ratio of Gd / Zn) and the ageing temperatures have a significant effect on the precipitation path of Mg-Gd-Zn alloys. Recently, the LPSO structure has been reported in a Mg-15Gd-0.8Zn-0.8Mn alloy (wt %) and was investigated using energy dispersive X-ray spectroscopy (using the Cliff-Lorimer k-factor method for quantification) [11]. It was found that the LPSO structure consists of Gd- and Zn-enriched solute clustering, indicating that there is a significant co-segregation of Gd and Zn within the LPSO structure. However, no

significant Mn was observed in the LPSO structure within experimental uncertainty of the measurement (~0.1%). This is surprising as the addition of Mn has been reported to promote the formation of the LPSO structure in the Mg-15Gd-1Zn-0.4Mn alloy [12]. Further development of these high performance Mg alloys is being held back by a lack of a thorough atomic scale characterization of the LPSO structures. Such information is essential to support theoretical modeling and elucidate precipitation mechanisms.

In this paper, we apply atomic scale high angle annular dark field scanning transmission electron microscopy (HAADF STEM) imaging and electron energy loss spectroscopy (EELS) to elucidate the elemental distribution (i.e. Gd, Zn and Mn) within the LSPO structure in the Mg-15Gd-0.8Zn-0.8Mn alloy (wt %). This investigation is of great necessity for the development of high performance Mg alloys because of the fact that a high ductility can be achieved by tailoring LPSO structure and thereby by the activity of non-basal $\langle a \rangle$ slip [12, 13].

2. Materials and Methods

The Mg-15Gd-0.8Zn-0.8Mn alloy (wt %) is referred to commercially as EZM1511. The EZM1511 alloy was prepared from pure Mg (99.9%), Zn (99.9%) and Mg-28Gd in an electric resistance furnace under the protection of an anti-oxidizing flux (55 % KCl, 15 % BaCl₂, 2 % MgO, 28 % CaCl₂), and then cast into a sand mould. The sand is mixed with sodium alkyl sulfonate mould, 0.25-1% S and 0.2-0.5% H₃BO₃ in order to protect the Mg alloy during casting. Mn was added using MnCl₂. Casting temperature is about 720 °C.

The as-casting sample is about 12 mm in diameter and 160 mm in length. Solution treatment was performed at 520 °C for 1000 h, followed by quenching into cold water.

Thin foil samples suitable for transmission electron microscope (TEM) and STEM imaging were prepared using a Gatan Precision Ion Polishing System (PIPS, Gatan model 691). The samples were mechanically ground, polished and dimpled to about 30 μm in thickness, and then ion-beam milled until electron transparent. The preparation temperature was kept constant at about -10 °C using a cold stage during ion beam polishing.

Conventional TEM imaging and diffraction was performed using a Philips CM12 microscope operated at 120 kV equipped with a CCD-camera (GATAN Model 794 MSC BioScan). HAADF STEM imaging and EELS were performed using a Nion UltraSTEM100 aberration corrected dedicated STEM. The microscope was operated at an acceleration voltage of 100 kV and an electron probe convergence semi-angle of 31 mrad, which resulted in an estimated minimum electron probe size of 0.08 nm. The cold field emission gun of the microscope has a native energy spread of 0.35 eV. The HAADF detector collection semi-angle was 83 - 185 mrad and the spectrometer collection semi-angle was 36 mrad. EELS elemental maps were then created by integrating the EELS signal of each edge (at a nominal edge onset energy): Gd $M_{4,5}$ (1185 eV), Zn $L_{2,3}$ (1020 eV), Mn $L_{2,3}$ (640 eV), Fe $L_{2,3}$ (708 eV), Mg K (1305 eV) and O K (532 eV), over a suitable energy window after subtracting the preceding exponential background fitted with a power law. All EELS edges were identified following reference [14]. EEL spectra were de-noised using Principal Component Analysis (PCA) as implemented in the MSA plugin for [15] for Gatan's Digital Micrograph software. The intensities of the EELS

maps were displayed on a false colour scale, so that within each map, a low intensity (black) corresponds to a lower relative concentration, while increased contrast (colour) corresponds to an increase in (relative) elemental concentration.

3. Results

Figure 1 shows bright field TEM micrographs (Figure 1a, c) and corresponding selected area electron diffraction (SAED) patterns (Figure 1b, d) of the LPSO structure in the EZM1511 alloy. A significant density of areas displaying the LPSO structure was observed along grain boundaries (Figure 1a) and within the Mg matrix (Figure 1c). In the SAED patterns (Figure 1b, d), fourteen consistent diffraction spots attributed to the LPSO structure are present at regular intervals between the transmission spots ($\{0000\}$) and diffraction spots corresponding to the $\{0002\}$ planes of the Mg matrix. The LPSO structure can, therefore, be indexed to be of a “14H type”.

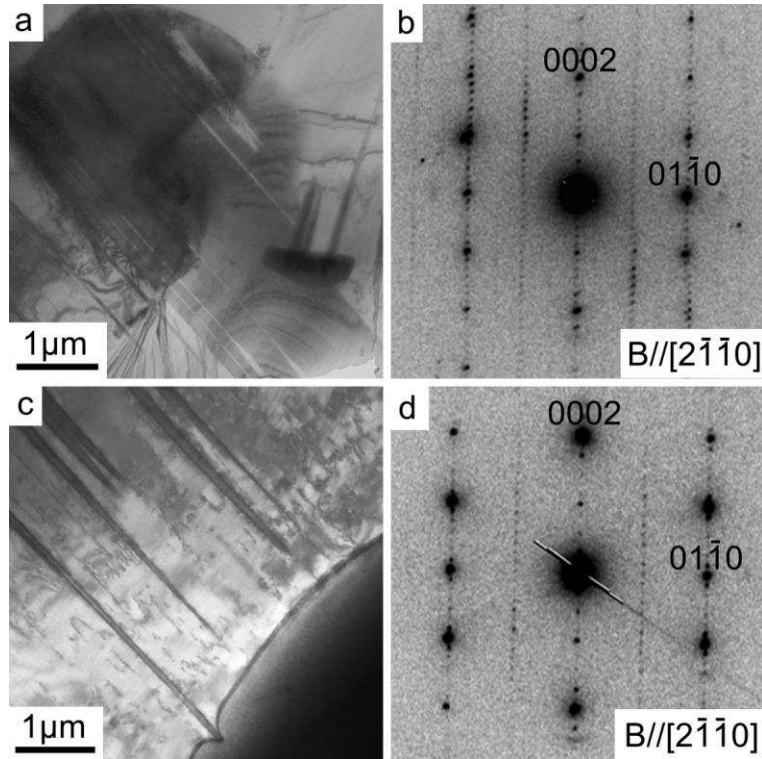


Figure 1: Bright field TEM micrographs (a, c) and corresponding selected area electron diffraction (SAED) (b, d) patterns showing the LPSO structure in the EZM1511 alloy. The electron beam is parallel to $[2\bar{1}10]_{\text{Mg}}$.

Figure 2 shows a HAADF-STEM micrograph viewed in a $[2\bar{1}10]$ zone axis projection (Figure 2a) and its Fourier transform (FFT) (Figure 2b) taken from the region of the Mg matrix shown in Figure 2a where a single instance of the LPSO structure was identified. Figure 2c shows the HAADF-STEM image and EELS elemental maps of Zn, Gd, Mg, O and Fe for the rectangular region highlighted in Figure 2a revealing the elemental distribution of the LPSO structure in the EZM1511 alloy. The atomic resolution images reveal that the LPSO phase is about two atomic layers in thickness (Figure 2a), while the chemical maps show it is enriched with Gd and Zn (Figure 2c), which is fully consistent with previous work [11]. It should be noted here that trace amounts Fe and O were

observed, which can be attributed to the impurity of the raw materials used and oxidation (through exposure of the samples to air during handling), respectively.

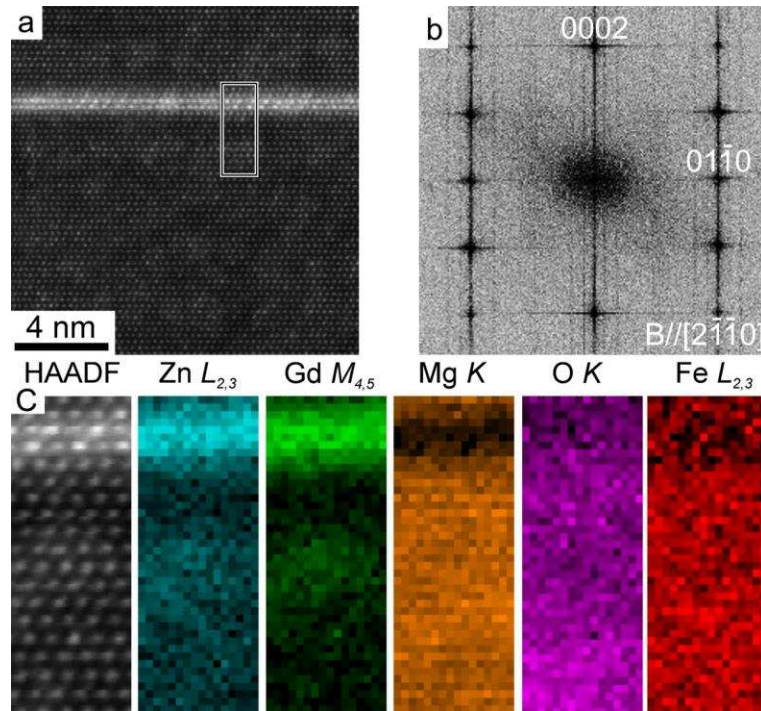


Figure 2: (a) HAADF-STEM micrograph, (b) Fourier transform (FFT) taken from the region of the Mg matrix in (a), (c) HAADF-STEM image and EELS elemental maps of Zn, Gd, Mg, O and Fe showing the elemental distribution within the LPSO structure in the EZM1511 alloy. The electron beam is parallel to $[2-1-10]_{\text{Mg}}$.

Figure 3 shows an “overview” HAADF-STEM micrograph (Figure 3a), a “close up” HAADF-STEM micrograph (Figure 3b), as well as a HAADF-STEM image and EELS elemental maps of Zn, Gd, Mg, O and Fe (Figure 3c) of a multi-LPSO structure (multi-layers) of a type frequently observed along the grain boundaries in the EZM1511 alloy. As in the single LPSO structure (Figure 2), each of the separate LPSO structures is approximately two atomic layers in thickness (Figure 3a, b) and is enriched with Gd and Zn (Figure 3c). The single layer LPSO structure has been related to stacking faults [12],

which may further convert into LPSO structure (multi-layers) due to a very long annealing time at elevated temperatures (520 °C for 1000 h in this study). Indeed, the LPSO structure in the bottom of Figure 3a is well ordered while the LPSO structure on the top of Figure 3a appears to be not well-ordered yet. However, a consistent enrichment of Gd and Zn within the LPSO structure can be seen in both cases. Importantly, no Mn enrichment of the LPSO structure was observed in either case within measurement accuracy.

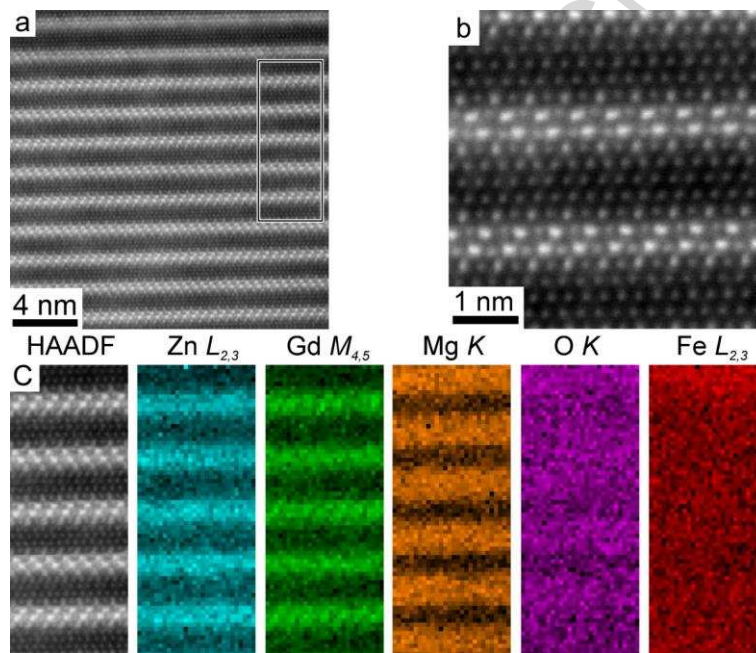


Figure 3: (a) HAADF-STEM micrograph, (b) Higher magnification HAADF-STEM micrograph of the same area, (c) HAADF-STEM image and EELS elemental maps of Zn, Gd, Mg, O and Fe showing the elemental distribution within the LPSO structure in the EZM1511 alloy. The electron beam is parallel to $[2-1-10]_{\text{Mg}}$.

In order to further verify the Mn distribution, Figure 4 shows a single spectrum averaged over the entire region shown in the HAADF image to the right. While a very weak Mn signal was resolved, no significant variations in Mn signal were observed over this region,

suggesting that Mn is indeed present but its concentration may be beyond the detection limitation of HAADF-STEM and EELS. Mn is known to have a limited solubility (about 0.4 at % at 520 °C) in the Mg matrix [16], and the very low signal levels detected here would be consistent with such low content. This reveals that Mn may not be directly involved in the formation of the LPSO structures, although it does not rule out the possibility that the presence of Mn within the Mg matrix may decrease the stacking fault energy required for the formation of the LPSO structure [12]. Further atomic scale characterization of Mn distribution using experimental techniques with lower detection limits for trace elements, such as atom probe tomography, and atomic scale simulation using density functional theory is still required to understand the formation mechanism of the LPSO structure in Mg-Gd-Zn-Mn alloys.

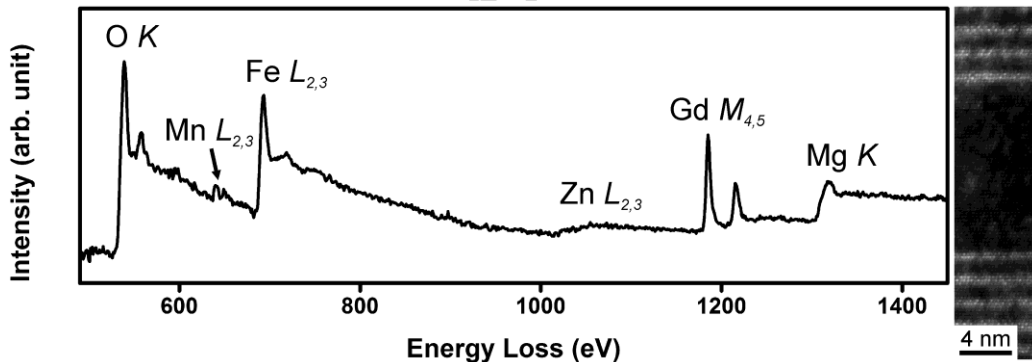


Figure 4: A single averaged spectrum taken from the entire region showed in the HAADF image (right). Note that a very weak Mn signal was resolved but no significant variations in Mn signal were observed within the probed region. The electron beam is parallel to $[2-1-10]_{\text{Mg}}$.

4. Conclusions

We have investigated the elemental distribution of the LPSO phases in a Mg-Gd-Zn-Mn alloy by atomic scale HAADF-STEM imaging and EELS. While enrichment of Gd and

Zn was observed within the LPSO structure, no accompanying Mn enhancement was observed. After averaging over a large region, a very weak Mn signal was resolved but no significant variations in Mn signal were observed over this region, suggesting that Mn is indeed present. The results of the present study might provide useful information to inform modelling and support the development of high performance Mg alloys.

Acknowledgments

The author (J.H. Li) acknowledges the casting sample preparation from Shanghai Jiaotong University, the access to TEM instruments at the Erich Schmidt Institute of Materials Science of the Austrian Academy of Science and the financial support from the Major International (Regional) Joint Research Project (No. 51420105005) from China and the projects (EPU 09/2016, CN 09/2016, mmc-kf15-11). The SuperSTEM Laboratory is the U.K. National Facility for Aberration-Corrected Scanning Transmission Electron Microscopy, supported by the Engineering and Physical Sciences Research Council (EPSRC). SJH and XLZ thank EPSRC for funding under grant EP/M010619/1.

References

1. B. Smola, I. Stulíková, F. von Buch, B.L. Mordike, *Mater Sci Eng A* 324 (2002) 113-117.
2. J.F. Nie, *Metall. Mater. Trans. A* 43 (2012) 3891-3939.
3. E. Abe, Y. Kawamura, K. Hayashi, A. Inoue, *Acta Mater.* 50 (2002) 3845-3857.
4. E. Abe, A. Ono, T. Itoi, M. Yamasaki, Y. Kawamura, *Philo. Mag. Let.* 91 (2011) 690-696.
5. M. Yamasaki, M. Matsushita, K. Hagihara, H. Izuno, E. Abe, Y. Kawamura, *Scr.Mater.* 78 (2014) 13-16.
6. J.F. Nie, X. Gao, S.M. Zhu, *Scripta Mater.* 53 (2005) 1049-1053.
7. J.F. Nie, K. Oh-ishi, X. Gao, K. Hono, *Acta Mater.* 56 (2008) 6061-6076.
8. Z. Li, J.X. Zheng, B. Chen, *Mater. Charact.* 120 (2016) 345-348.
9. M. Yamasaki, M. Sasaki, M. Nishijima, K. Hiraga, Y. Kawamura, *Acta Mater.* 55 (2007) 6798-6805.
10. J.F. Nie, B.C. Muddle, *Acta Mater.* 48 (2000) 1691-1703.
11. J.H. Li, M. Albu, Y.J. Wu, L.M. Peng, M. Dienstleder, G. Kothleitner, F. Hofer, P. Schumacher, *Advanced Engineering Materials*. DOI: 10.1002/adem.201600705
12. W. Rong, Y. Zhang, Y.J. Wu, M. Sun, J. Chen, Y. Wang, J.Y. Han, L.M. Peng, H.X. Ding, *J Alloy Compd.* 692 (2017) 805-816.
13. R. Chen, S. Sandlöbes, X.Q. Zeng, D.J. Li, S. Korte-Kerzel, D. Raabe, *Mater Sci Eng A* 682 (2017) 354-358.
14. C.C. Ahn, O.L. Krivanek, *EELS Atlas*, Warrendale, Gatan Inc, 1983.

15. M. Watanabe, M. Kanno, D. Ackland, C. Kiely, D. Williams, *Microscopy and Microanalysis* 13 S2 (2007) 1264.
16. J. Gröbner, D. Mirkovic, M. Ohno, R. Schmid-Fetzer, *JPEDAV* 26 (2005) 234-239.

ACCEPTED MANUSCRIPT

Highlights

1. Gd and Zn enrichment was observed within the LPSO structure in an Mg-15Gd-0.8Zn-0.8Mn (wt %) alloy
2. No significant enrichment in Mn was observed within the LPSO structure.
3. These results provide useful information to support the future development of high performance Mg alloys.

ACCEPTED MANUSCRIPT